Proceedings of the 17th Pan-American Conference on Soil Mechanics and Geotechnical Engineering (XVII PCSMGE), and 2nd Latin-American Regional Conference of the International Association for Engineering Geology and the Environment (IAEG), La Serena Chile, 2024.

Distributed Fiber Optic Sensors – Applications to Geological Engineering and Civil Infrastructure

Sensores Distribuidos de Fibra Óptica - Aplicaciones para la Ingeniería Geológica y la Infraestructura Civil

Siyu Lu and Dante Fratta
Geological Engineering, Civil and Environmental Engineering, University of Wisconsin-Madison, USA (slu222@wisc.edu and fratta@wisc.edu)

Esra Ak
General Directorate of Mineral Research and Exploration, Turkish Geological Survey, Ankara, Turkey

Herb Wang
Geoscience, University of Wisconsin-Madison, USA

ABSTRACT: Sensing arrays developed from interpreting the interaction of laser pulses within fiber optics revolutionize how we measure and assess natural and built environments. Fiber-optic-based measurement techniques monitor temperature, strains, and vibration with arrays as long as tens of kilometers with temporal sampling rates higher than 1 kHz, spatial separation of 1 m or more minor, and sensing lengths of about 2 m with fine temperature and strain resolutions. These techniques yield challenges and opportunities for several areas of science and engineering, including geotechnical engineering. We used these sensing arrays to monitor the performance of low-temperature geothermal fields, measure strains and stresses in hard rock mines, sense surface and body waves in alluvial formations, and capture signals from traffic noise. All these applications are inherent in geological engineering and civil infrastructure. This paper reviews the application and challenges of using fiber optic-based distributed acoustic sensing arrays for monitoring the engineering infrastructure and geotechnical engineering systems. We explore advances and limitations of using sources of opportunities such as ambient noise and traffic signals to monitor the response of infrastructure systems and to collect data for imaging the near subsurface.

KEYWORDS: *DAS, strain, strain rate, vibration in soils, distributed sensing arrays*

1 INTRODUCTION.

Low-loss optical fiber is a medium for long-distance communication. The technology's maturity allows optical fibers to carry more information, laying a solid foundation for optical fiber sensing technology. One significant advantage of optical fiber sensing is its real-time, continuous measurements along large fiber sections, making it ideal for large urban projects such as monitoring dams, bridges, and buildings. These measurements are compatible with geological engineering measurements and civil infrastructure sensing. Fiber-optic-based techniques can provide high temporal (higher than 1 kHz) and spatial (less than 1 m) resolutions and extended reach (up to 100 km), providing optical fiber sensing advantages over other sensors (McDaniel et al., 2018; Lindsay et al., 2020). Furthermore, optical fiber has good chemical stability and is relatively insensitive to electromagnetic interference (Zhang et al., 2018). These advantages make it ideal for application in areas with higher safety requirements, such as aerospace system navigation (Pierce et al., 1996; Okabe et al., 2016; Breslavsky et al., 2017), oil and gas field monitoring (Clowes et al., 1999), mine monitoring (Zeng et al. 2022a; Cunningham et al., 2023), and monitoring dams, bridges, large buildings (Masciotta et al., 2018). This article discusses current challenges and potential applications in optical fiber sensing technologies in near-surface imaging and civil infrastructure system monitoring.

1.1 *Distributed Fiber Optic Sensing Technology*

The interaction of laser pulses with imperfections in the silica of optical fiber forms a string of sensors in the distributed sensing arrays. Distributed Temperature Sensing (DTS), Distributed Strain Sensing (DSS), and Distributed Acoustic Sensing (DAS) use information encoded in backscatter events caused by incident laser pulses at 1550 nm wavelengths with imperfections in the silica core to sense properties around the fiber. The techniques interpret Raman (DTS – Selker et al. 2006), Brillouin (DSS and DTS – Güemes et al. 2010), and Rayleigh (DAS – Parker et al. 2014) scattering events to assess the physical field changes along the fiber length. The location of the fiber's physical change is determined using Optical Time Domain Reflectometer (OTDR) concepts. By knowing the speed of light in the fiber and the time the laser pulse takes from being emitted to the arrival of a backscattered signal,

the location of the scattering event along the fiber is precisely determined, forming distributed fiber optic sensing techniques.

With measurement resolutions as fine as 0.01°C, DTS is suitable for applications where temperature changes must be closely monitored. Meanwhile, DSS and DAS techniques monitor pseudo-static and dynamic strain sensing. Thus providing versatile solutions for monitoring temperature, strain, and acoustic disturbances or vibrations along the fiber. The choice between DTS and DSS/DAS depends on the specific requirements of the monitoring application, whether it involves temperature-sensitive processes or the need to detect strains or vibration events in the environment. While DTS and DAS can be used independently as dynamic strain and temperature are uncoupled phenomena, it is good practice to sense both pseudo-strain and temperature when deploying DSS to separate thermal and mechanical strains from the fiber measurements. There is another difference between DTS and DSS/DAS response, and it is related to the fact that temperature is not a vector magnitude while normalized deformation (i.e., strain) is. So, while DTS does not show directionality, DSS and DAS respond mainly in the direction of the fiber (Mateeva et al., 2014). As DSS and DAS are techniques that tend to overlap in their applications, their difference is related to frequency responses; we will focus on DAS for infrastructure and geological engineering applications.

1.2 *Applications of Fiber Optic Sensing in Civil Infrastructure*

The main applications of distributed fiber optic measurements in civil infrastructure are transportation, energy, and construction. DAS can be used for rail transit to determine real-time train location information (Ferguson et al., 2020). The technique can monitor intrusions along the railway lines, assess rail track conditions, and respond to traffic. By training machine learning algorithms, DAS measurements help identify events that conform to time patterns and ensure railway traffic safety (Li et al., 2020). Embedding new fiber specifically can be costly for monitoring the condition of operating rail and roads. However, deploying new fiber during construction (Hubbard et al., 2022) or interrogating dark optical fibers (i.e., fiber not operational by telecommunication companies also reduced installation costs - Lindsey et al., 2020). Recorded signal statistics with fiber tend to be anonymous, reducing privacy concerns.

The primary purpose of using DAS and DTS in bridge and tunnel engineering is to test the stability of the structure. Optical fiber can realize long-time, long-distance detection on the reinforced concrete bridge deck or monitor fire hazards inside tunnels. Its application has been demonstrated through static load comparison experiments of bridge beams, and the local stress measured by the stress meter is consistent with the DAS results (Zhu et al., 2019).

DTS has found applications in downhole monitoring of oil and gas fields and is used in transmission lines, pipelines, boreholes, etc. (Taminola and Hill, 2009). DTS arrays track high-voltage transmission cables by measuring their thermal profile, where abnormal temperature increases are associated with faults in parts of transmission lines. This feature allows DTS to detect problems and repair and replace them before they cause real damage. In addition, DTS is especially suitable when the temperature of the transported gas is different from that of the external gas (Yokogawa, 2013). In environmental studies, DTS has been deployed to monitor temperature anomalies and assess fire conditions in the field (Cram et al., 2016). The distributed nature of the methodology allows for the quantification of forest fire in areas where the vegetation bed is heterogeneous and, therefore, difficult to evaluate and locate.

1.3 *Applications of Fiber Optic Sensing in Geological Engineering*

DTS arrays are used in a geothermal reservoir area. The thermal responses of sediments and rocks near the surface can be understood by observing temperature changes in time and across the volume of geothermal fields (Patterson et al., 2017). Suppose the optical fiber is placed along the borehole wall. In that case, it can monitor the geothermal gradient in the formation and provide the basis for understanding the borehole field's heat exchange potential, allowing operation for the efficient production of geothermal power (McDaniel et al., 2018; Hegg et al., 2024). In addition, the fluid properties of rocks and pore water also affect near-surface temperature changes. In the underground heat exchange system, groundwater flow helps dissipate heat exchange quickly. This response can be monitored by deploying DTS fiber inside and outside bore fields.

In near-surface measuring applications, optic fibers are suitable as a passive method for soil moisture measurements. For example, Dong and other researchers proposed using the Adaptive Particle Batch Smoother Algorithm (APBS) to obtain a high-resolution (1 m) soil moisture distribution map (Dong., 2016). In contrast, the active measurement uses cable heating to determine the thermal conductivity of soil and invert for soil moisture (Cao et al., 2016). Measurements of soil moisture using electric pulses of coaxial heating can also achieve a resolution of 1m over optical cables more than 10,000 m long (Sayde et al., 2010).

DAS is also used in geological studies to detect structural or lithological features. For example, DAS can be used to map vertical seismic wave profiles (Mateeva et al., 2014), achieve extensive reservoir imaging (Harris et al., 2017), monitor the variation of seismic wave propagation velocity at shallow surfaces (Fang et al., 2020). In Reykjanes Peninsula in Iceland, a 15 km long DAS array collected seismic waves and ambient noise signals that were then used to image faults (Jousset et al., 2018). The fault zone appeared as an area of lower wave velocity and presented phase changes. Traditional seismometers collocated along the DAS array showed high coherence levels. Additional experiments have also demonstrated the similarity between DAS and geophone data in the same location waveform (Lindsey et at., 2017; Castongia et al., 2017; Wang et al., 2020). Castongia et al. compared the first arrival times collected with geophones and a DAS array in frozen Lake Mendota in Madison, Wisconsin, USA, and showed only minor differences in delay. Wang et el. (2020) reported that the results of co-located nodal seismograph and DAS arrays in Brady Hot Springs, Nevada, showed similar results. The two arrays capture the seismic waves caused by an ML 4.3 earthquake with an epicenter 150 km away. The DAS and seismometer arrays in the same area show similar strain waveforms for the arrival of P and S-waves.

In addition to active sources, such as common earthquakes (Fang et al., 2020) and active sources (Yu et al., 2019; Lecocq et al., 2020), other passive sources such as ambient noise (Dou et al., 2017; Cheng et al., 2021) and thunder-induced seismic waves (Zhu et al., 2019) can also be used in some areas where earthquakes are not active enough.

Finally, researchers have been shifting to using dark fibers to study a wide range of shallow marine sediment characteristics. The diverse environmental noise sources in the ocean also provide conditions for studying ocean dynamics (Lindsey et al., 2019). In particular, spectral analysis of surface waves (SASW) and multichannel analysis of surface waves (MASW) can be used to interpret DAS data. After the dispersion curves are extracted, several approximate formation models are modeled forward to obtain multiple theoretical dispersion curves. Then, an inversion is completed by comparing the actual and empirical dispersion curves. The refraction microtremor (ReMi) method is similar to MASW but mainly uses microseismic data generated by ambient noise (Louie, 2001). Ambient noise has a low signal-to-noise ratio. Longer time signals can be recorded and stacked to compensate for providing a higher-quality dispersion curve. SASW and MASW can map the stiffness of different dimensions with varying numbers of channels as receivers.

2 LOCATION AND METHODS

2.1 Garner Valley DAS Deployment

Our research team installed a DAS array along California Highway 74 in Garner Valley, Southern California. The University of California-Santa Barbara initially operated the site. The site benefited from detailed geological studies using Spectral Analysis of Surface Waves (SASW – Stokoe et al., 1994) and boreholes (Youd et al., 2004). At the site, we laid a 762-m fiber optic cable in a 0.3 m to 0.4 m deep trench, and we coupled the cable to the ground by covering and lightly compacting the excavated material. The array comprised two 160-m long lines (Long Line I and Long Line II) mainly parallel to the highway, two 80-m long lines perpendicular to it (Short Line I and Short Line II), and two additional diagonal segments (Cross Line I and Cross Line II) meeting at the midpoint of the long line close to the road (Figure 1 – Lord et al. 2016).

We deployed this optical fiber to assess the capabilities of DAS arrays for high spatial sensing in near-surface physical imaging. During the original study, we excited the array using three different vibroseis while utilizing traffic and ambient noise as passive signal sources. This paper uses the data from the vibration from vehicles near the DAS cable and the strain generated near the surface to detect vehicle traveling events further away from the cable. We deployed filters to highlight the vibrations caused by the cars and distinguish those parts from ambient noise. Using data from successive DAS channels rather than single point receivers at start and end points helps assess different traffic patterns: number of vehicles, type of vehicles, speeds, roadway quality, etc. (Lancelle, 2016; Ak, 2019).

2.2 *Data processing*

This study presents two studies on potential applications of fiber optic DAS arrays for monitoring the infrastructure and imaging the near surface. We analyzed data from multiple groups of vehicles passing through the das array detection section. We examined those results to assess conventional traffic flow, including the number of cars and the speed estimation. Using these data, we also compare multiple vibration patterns that repeatedly occurred when vehicles passed through similar locations to locate transverse cracks and potholes in the roadway. These analyses allow imaging of roadway imperfections that may cause a reduction in rider comfort and are an indication of repair needs. During traffic monitoring, the surface wave speed range could be determined. So, then we used cross-correlation processing on the signals caused by traffic and ambient noise to obtain dispersion curves of surface waves to the image near the surface.

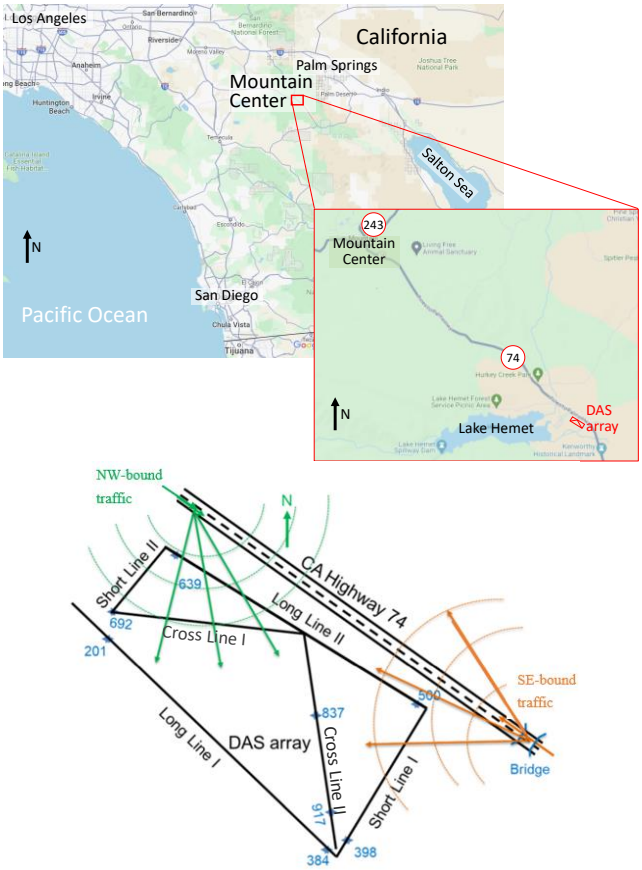

Figure 1. Geographic location and a sketch of the DAS array study area at Garner Valley site (33°40'06.76" N, 116°40'24.53" W). The blue numbers indicate the DAS channel number within the array, and each array segment is labeled.

3. RESULTS

3.1 *Traffic and Road Conditions Monitoring*

DAS channels parallel to the highway (i.e., channels 500 through 640 – Figure 1) are used for traffic monitoring studies. We call channels 500 and 640 gates for vibration signals and use them to indicate when vehicles enter or exit the monitored section of the road. The collected data were then evaluated to achieve the following parameters/processes:

- *Vehicle counting and car speeds*: A transverse crack at the southeast end of the array (channel 500) and another crack at the northwest (channel 640) serve as gates to the passing traffic. We

use signals at those gates to count vehicles, determine their directions, and calculate average speeds (Figures 2 and 3).

- *Car weights and sizes*: Vehicle weight and length differences result in different wave signatures. The vehicle's weight can be sensed and compared in terms of amplitude. For cars traveling at similar speeds, heavier vehicles passing through the same imperfection produce greater amplitudes than lighter vehicles (Figure 4). Similarly, because of the more considerable distances between the front and rear axles of trucks, the vibration of each pair of wheels can be individually detected when it hits an imperfection of the roadway. It is necessary to distinguish whether signatures are generated by the front and rear wheels of the exact vehicle or by two close vehicles driving in the same direction. Vehicle speed, spacing, and the car's position relative to the DAS fiber are considered to achieve this goal.

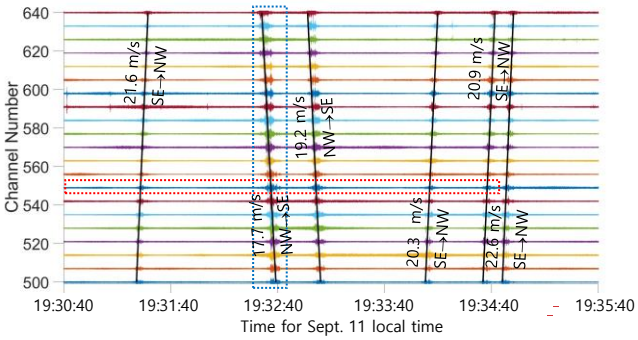

Figure 2. Counting vehicles. Each black line represents one event that a car travels through the detected area. The data in the blue and red rectangles are later used in Figures 3 and 4.

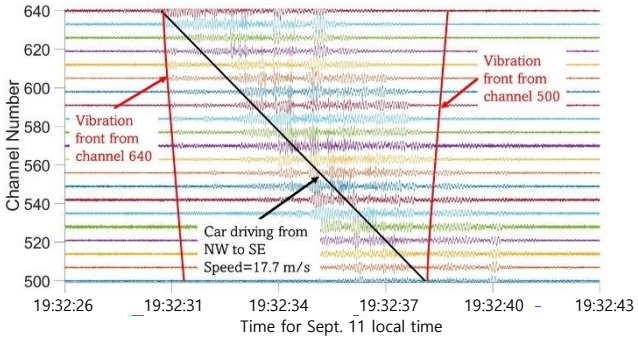

Figure 3. Analysis of car speeds in DAS data (blue rectangle in Figure 2). The black line represents a vehicle's rate of travel. The time difference between the two red lines and the distance between channels 500 and 640 are used to calculate the car speed. The two red lines are the moveouts from local imperfections near channel 500 and near channel 640 fit with a 220 m/s wave speed.

- *Seismic wave velocity*: Since the channel separation in the DAS array is one meter and the channels' position concerning the highway is known, the moveout times from multiple imperfections on the roadway surface are used to calculate the seismic wave propagation speed (Figure 3).

- *Evaluating the road surface conditions*: The transversal cracks, bumps, and potholes along the road surface generate point seismic sources radiating energy in every direction when a vehicle hits them (Figure 5). The channel with the highest amplitude and the shortest arrival time is closest to surface imperfections, while the moveout responses' slope captures the surface soil's wave speed. However, since vehicles may shift wheel paths, the actual number of imperfection sources indicates the quality of the roadway surface. The greater the number of moveout curves, the worse the road condition of that section. Cracks and potholes outside the monitoring section can also be studied, but these imperfect events appear as constant moveouts in the vibration records. Suppose the crack or pothole producing the vibrations is inside the monitoring section. In that case, it will appear as a hyperbola in the DAS record, with the lower travel time corresponding to the closest channel (Figure 5). So, we use the vibrations caused by roadway imperfections to image the quality of the surface. However, these road imperfections might have different sizes and shapes. Large transverse cracks may run through the entire road surface, while minor portholes may affect only part of the roadway. Therefore, to get a more specific understanding of road damage, comparing the incidents of same-direction vehicles passing through the same section is necessary.

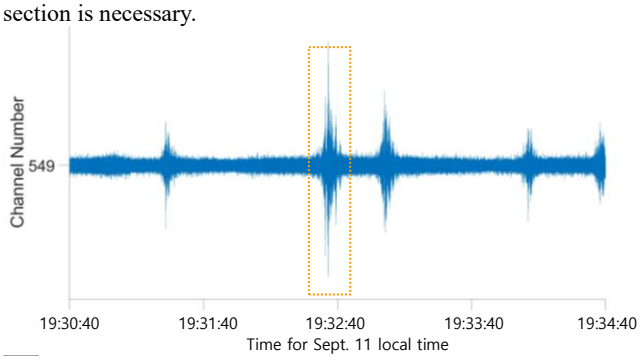

Figure 4. The example shows that car weight or size differences cause differences in waveform. The rectangle indicates the presence of a heavier vehicle car traveling through the selected channel. (as shown in Figure 2).

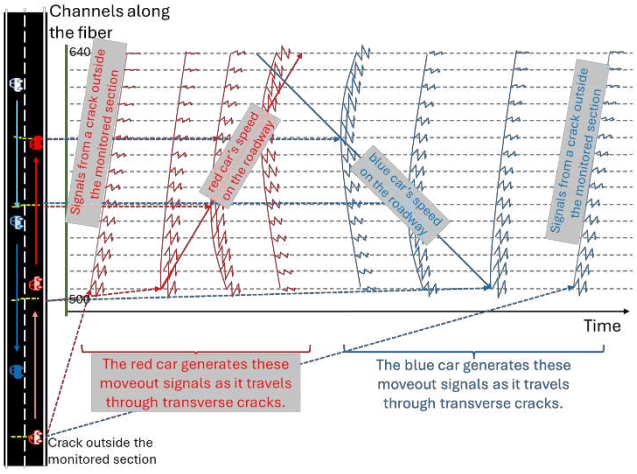

Figure 5. Interpret traffic data to assess wave propagation speed, vehicle driving direction, speed, and roadway surface properties.

Our section of highway is an undivided road with two lanes. Differences in traffic mainly reflect directions and vehicles' speeds

and sizes (Figure 2). So, traveling vehicles cause vibration with different signatures even when passing through the same damaged section of the road. These differences become more evident in multi-lane highways. The general trend is that larger vehicles cause higher amplitude vibrations (Figure 4). The time difference between axles can also determine sizes. Longer vehicles usually have clearer time gaps between multiple wheels' traces. Heavier vehicles generate more deformation of the highway surface and cause more significant amplitude signals. Changes in velocity over short periods and short distances can also lead to mislabeling of imperfection locations. This positional shift may be considered as different branches of the fracture. However, we could not control all these factors during the processing process.

Under ideal contrast conditions, the vibration waveform of two vehicles running in the same direction and passing over a road imperfection would appear at different times. The vibration event may appear or disappear in isolation during a vehicle's passing, indicating that the damage was minor and did not continuously cut off the road. However, in the collected data, the distribution of damaged areas on the road is not uniform, and multiple vehicles travel close to each other, causing vibration signals from various cars to overlap (Figure 6). For example, the superposition of such waves causes constructive or destructive interference, which makes it difficult to identify single waveforms within the waveform. Therefore, a deconvolution script might be needed to interpret waveforms further and improve road damage imaging.

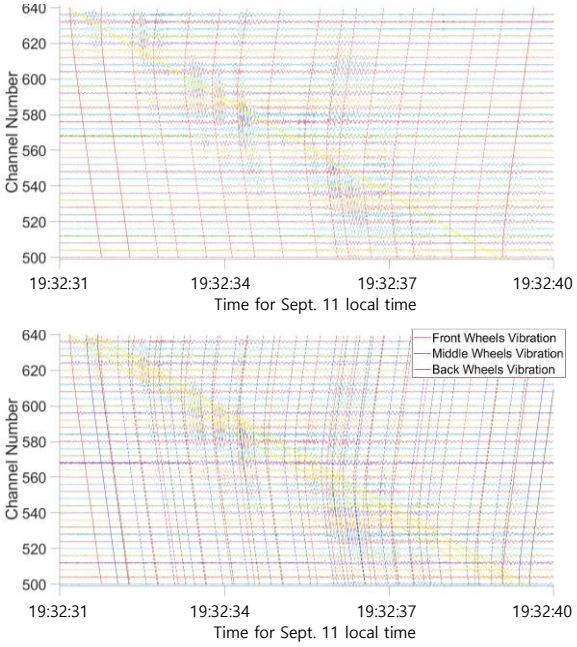

Figure 6. Vibration sources along the roadway determine road conditions. Dash lines represent moveouts from imperfections inside the array length (Some vibration fronts are ignored for better display). The three yellow lines indicate the position of the vehicle's front, middle, and rear wheels. Red, blue, and black lines represent the vibration fronts caused by the front, middle, and rear wheels.

Monitoring consecutive channels can identify most traffic events by analyzing the DAS strain rate response. Then, the identification of simultaneous events in different directions is relatively simple because the waves generated by the vibration of vehicles when they drive into different regions have different propagation directions. However, it is difficult to identify vehicles traveling in the same direction simultaneously as the vibrations generated by one vehicle's wheel may interact with those caused by another. Single vehicles provide information on common imperfections when those imperfections positions appear in multiple vehicles driving simultaneously, using several recognizable vibration wave positions; the time when the car enters or exits the array range can be simulated. The information on vehicle speeds and driving directions in different periods is recorded and summarized in Table 1). The total number of vehicles is 259, and traffic flow is significantly higher in the period before 19:00. The speed of most vehicles ranges between 15 m/s and 27 m/s. The wave propagation speed of the surface soil next to the road is about 220 m/s (Figures 3 and 5). According to the seismic wave data obtained, the vibration patterns caused by cars passing through imperfections or cracks on the monitoring road sections in different periods are consistent with each other in most cases. Although not every surface problem is fully captured in a single driving event due to the impact of the vehicle's wheel path, monitoring the overall road condition is still effective. Figure 7 and Table 2 summarize the location of cracks and potholes. The results presented in Figure 7 are compared to the transverse location documented in Google images. We used Google Earth images from 2011 to locate the transverse cracks, while our dataset was collected in 2013. So, the time difference between the year of labeling the cracks and data collection may explain the unobserved imperfections. Still, our analyses are consistent with the imperfections in the images overall.

Table 1. Time, direction, and velocity of traffic events (results for one 15-minute period example).

Time: 19:23:59-19:38:59					
Event Number	**Driving direction**	**Vehicle speed (m/s)**	**Event Number**	**Driving direction**	**Vehicle speed (m/s)**
1	NW to SE	18.4	10	SE to NW	21.6
2	NW to SE	20.6	11	NW to SE	17.7
3	NW to SE	21.5	12	NW to SE	19.2
4	NW to SE	25.9	13	SE to NW	20.3
5	NW to SE	18.4	14	SE to NW	20.9
6	NW to SE	19.4	15	SE to NW	22.6
7	SE to NW	17.9	16	NW to SE	23.3
8	SE to NW	21.9	17	NW to SE	24.1
9	SE to NW	25.9	18	SE to NW	21.5

3.1 *Evaluation of Dispersion Curves for the Evaluation of Dynamic Soil Properties*

We use 12 sets of 15-minute windows and six cable segments in different directions (i.e., Long Line I, Long Line II, Short Line I, Short Line II, Cross Line I, and Cross Line II – Figure 1) to evaluate dynamic soil properties. We initially applied a moving average and detrending to the collected data. We then conducted a cross-correlation analysis on 2-second time windows, comparing each channel with a designated channel at one end of the segment. The choice of this fixed reference channel is contingent upon the direction of the segment with respect to the highway: the reference channel is defined as the one nearest to the road. In the case of

Long Line I and Long Line II, sections parallel to the highway, the end, we arbitrarily selected the smallest channel number as the reference channel.

Table 2. Summary of transverse cracks and potholes positions on the road surface.

Time passing channel 500: 19:32:31.1					
Channel Number	Distance from channel 500 (m)	Vibration time after passing channel 500 (s)	Channel Number	Distance from channel 500 (m)	Vibration time after passing channel 500 (s)
500	0	0.00	594	94	5.30
509	9	0.51	603	103	5.81
517	17	0.96	613	113	6.38
523	23	1.30	620	120	6.77
530	30	1.69	628	128	7.22
536	36	2.03	630	130	7.34
545	45	2.54	634	134	7.56
553	53	2.99	640	140	7.90
557	57	3.22	Out of selected area	-13	-0.73
564	64	3.61		-25	-1.41
568	68	3.84		-28	-1.58
576	76	4.29		-40	-2.26
579	79	4.46		148	8.35
586	86	4.85		152	8.58

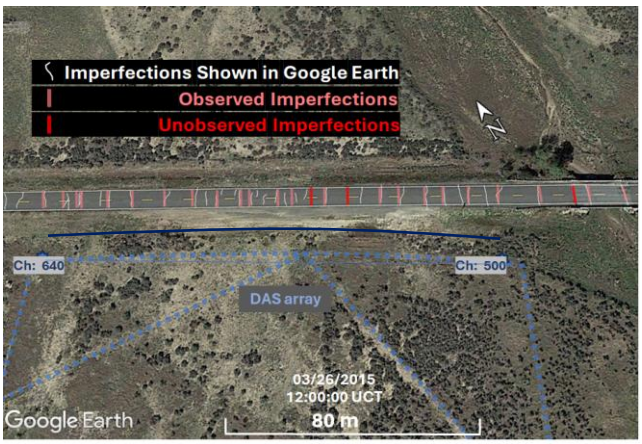

Figure 7. Location of transverse location on the roadway. The dark blue area corresponds to the DAS channels used in the analysis. The short white lines on the road represent the locations of road imperfections observed on Google Earth images. The short pink are vibration fronts having positions matching road imperfections. The three lines are vibration fronts not observed in Google Earth images.

The wave velocity of waves propagating in the direction away from the fixed reference channel is assigned a positive value. The cumulative cross-correlation results from each time window are stacked to reveal a shallow surface wave velocity of 200 m/s. However, the quality of the dispersion curves depends on the direction of the segment (Figure 8). The dispersion curves appear at 5 Hz and 15 Hz, with data from Short Line I and Short Line II showing at higher modes. Besides, those trends show a higher velocity distribution at higher frequency ranges as DAS arrays behave as low-pass filters with cutoff controlled by the wave velocity of the medium and the gauge length (Vantassel et al., 2022a; 2022b).

Our array captures distinct signals from ambient noise and traffic events. Due to the distinct amplitude differences between these signal sources, traffic events control the sum of the seismic wave amplitude absolute values across all channels. Separating different signal sources allows the grouping and separating other windows' effects with ambient noise and traffic for different channel segments. Figure 9 presents the dispersion curves of 150 minutes of data collected along Short Line I for three combinations of data sources. The quality of the dispersion curves decreases from using all the ambient noise and traffic signals together to just the traffic data and, finally, the ambient noise.

There are a few things to consider: (1) due to the short distance of the event to the fiber array and the energy created by the passing vehicles, the traffic data has a higher signal-to-noise ratio than the ambient noise data; (2) while the ambient noise has a lower signal-to-noise, it has a much larger number of time windows (the traffic events are localized in time and have shorted duration) allowing greater stacking numbers, and (3) the frequency content traffic signal is larger than the ambient noise. When considering these observations, the combination of ambient noise and traffic signals complement each other, improving the quality of the dispersion curve, as presented in Figure 9. These dispersion curves can then be used to image the dynamic properties of near-surface soils and sediments (e.g., Zeng et al., 2022b).

4. CONCLUSIONS

A 700-m, 2-dimensional DAS array is set up close to the California Highway 74 road in Garner Valley, Southern California. The ambient noise and traffic signal data collected by this array is used to access the highway infrastructure and local geological engineering properties. The number of vehicles, speed, direction of travel, type of vehicle, and degree of damage were assessed by analyzing the data. At the same time, the phase velocity dispersion of surface waves that reflect soil properties can be measured. The results show that the DAS array is feasible for traffic monitoring. Moreover, using different directions and source data can give a more comprehensive dataset that can be used to understand the near-surface dynamic properties of surface soils.

5. ACKNOWLEDGEMENTS

The data collection and analysis were initially supported by a National Science Foundation project under Award number CMMI 0900351 and by a U.S. Department of Energy (DOE) under Award Number DE-EE0006760. The Wisconsin Department of Transportation supports Ms. S. Lu. Silixa loaned the iDAS interrogator and their expertise for this study.

6 REFERENCES

Ak, E. (2019). Seismic Arrays for the Imaging of Alluvial Deposits and Monitoring Engineering Systems. Master's thesis, University of Wisconsin – Madison.

Breslavsky, D., Uspensky, V., Kozlyuk, A., Paschenko, S., Tatarinova, O., and Kuznyetsov, Y. (2017). Estimation of heat field and temperature models of errors in fiber-optic gyroscopes used in aerospace systems. Eastern-European Journal of Enterprise Technologies, 1(9-85), 44–53. URL: https://doi.org/10.15587/1729-4061.2017.93320.

Cao, D., Shi, B., Zhu, H., Zhu, K., Wei, G., and Gu, K. (2016). Performance evaluation of two types of heated cables for distributed temperature

sensing-based measurement of soil moisture content. Journal of Rock Mechanics and Geotechnical Engineering, 8(2), 212–217. URL: https://doi.org/10.1016/j.jrmge.2015.09.005.

Castongia, E., Wang, H.F., Lord, N., Fratta, D., Mondanos, M., and Chalari, A. (2017). An Experimental Investigation of Distributed Acoustic Sensing (DAS) on Lake Ice. Journal of Environmental and Engineering Geophysics, 22(2), 167–176. DOI: https://doi.org/10.2113/JEEG22.2.167.

Cheng, F., Chi, B., Lindsey, N. J., Dawe, T. C., and Ajo-Franklin, J. B. (2021). Utilizing distributed acoustic sensing and ocean bottom fiber optic cables for submarine structural characterization. Scientific Reports, 11(1), 5613. URL: https://doi.org/10.1038/s41598-021-84845-y.

Clowes, J., Edwards, J., Grudinin, I., Kluth, E. L. E., Varnham, M. P., Zervas, M., Crawley, C. M., and Kutlik, R. L. (1999). Low drift fiber optic pressure sensor for oil field downhole monitoring. Electronics Letters, 35, 926–927. URL: https://doi.org/10.1049/el:19990646.

Cram, D., Hatch, C., Tyler, S., and Ochoa, C. (2016). Use of Distributed Temperature Sensing Technology to Characterize Fire Behavior. Sensors, 16, 1712. URL: https://doi.org/10.3390/s16101712.

Cunningham, E., Lord, N., Fratta, D., Chavarria, A., Thurber, C. and Wang, H. (2023). Three-dimensional Distributed Acoustic Sensing at the Sanford Underground Research Facility. Geophysics. DOI: https://doi.org/10.1190/geo2023-0079.1.

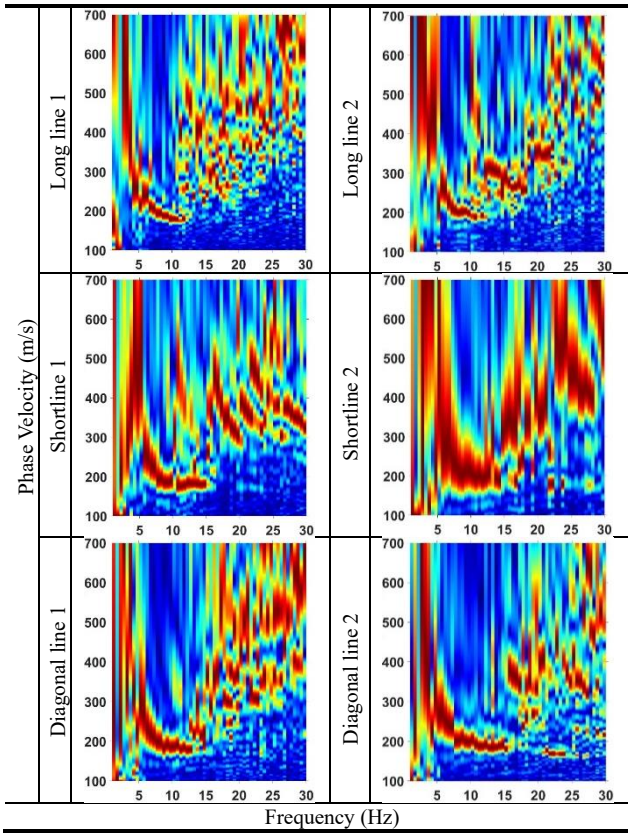

Figure 8. Dispersion curves using different direction cables using 180 minutes of data.

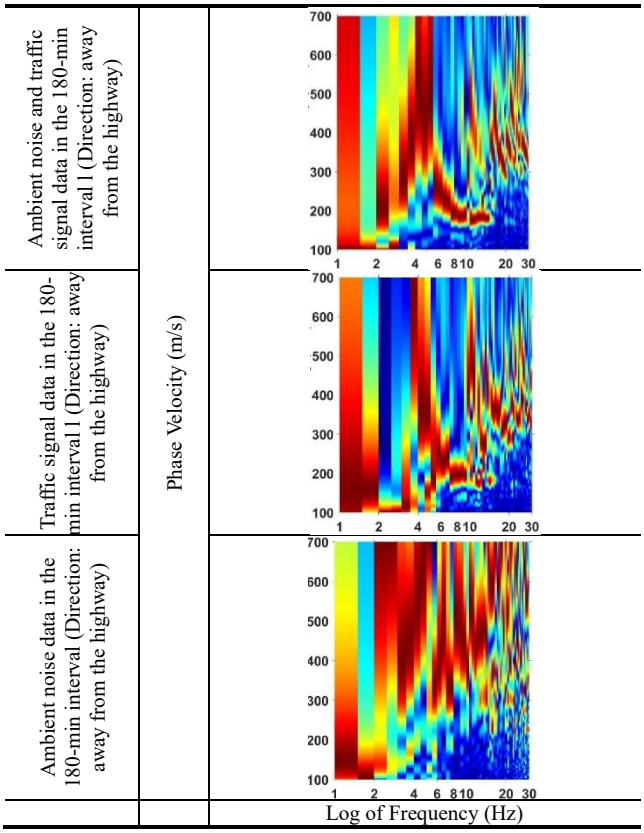

Figure 9. Dispersion for Shor Line 1 using different 2-second time windows with 180-minute recorded data (comparison between all ambient noise data, vehicle events data, and natural noise data).

Dong, J., Steele-Dunne, S.C., Ochsner, T.E., Hatch, C.E., Sayde, C., Selker, J., Tyler, S., Cosh, M.H., and van de Giesen, N. (2016). Mapping high-resolution soil moisture and properties using distributed temperature sensing data and an adaptive particle batch smoother. Water Resources Research, 52(10), 7690–7710. URL: https://doi.org/10.1002/2016WR019031.

Dou, S., Lidsey, N., Wagner, A., Daley, T., Freifeld, B., Robertson, M., Peterson, J., Ulrich, C., Martin, E., and Ajo-Franklin, J. (2017). Distributed Acoustic Sensing for Seismic Monitoring of The Near Surface: A Traffic-Noise Interferometry Case Study. Scientific Reports, 7, 11620. URL: https://doi.org/10.1038/s41598-017-11986-4.

Fang, G., Li, Y. E., Zhao, Y., and Martin, E. R. (2020). Urban Near-Surface Seismic Monitoring Using Distributed Acoustic Sensing. Geophysical Research Letters, 47(6), e2019GL086115. URL: https://doi.org/10.1029/2019GL086115.

Ferguson, R.J., McDonald, M.A.D., and Basto, D.J. (2020). Take the Eh? Train: Distributed Acoustic Sensing (DAS) of commuter trains in a Canadian City. Journal of Applied Geophysics, 183, 104201. URL: https://doi.org/10.1016/j.jappgeo.2020.104201.

Güemes, A., Fernández-López, A., and Soller, B. (2010), Optical Fiber Distributed Sensing - Physical Principles and Applications. Structural Health Monitoring 9(3), 233-245. DOI: https://doi.org/10.1177/1475921710365263.

Harris, K., White, D., and Samson, C. (2017). Imaging the Aquistore reservoir after 36 kilotonnes of CO2 injection using distributed acoustic sensing. Geophysics, 82(6), M81–M96. URL: https://doi.org/10.1190/geo2017-0174.1

Heeg, E., Tinjum, J.M., Fratta, D., Attri, S.D., Hart, D.J., and Luebbe, A.K. (2024). Quantifying the Long-Term Performance of a District-Scale Geothermal Exchange Field. 49th Workshop on Geothermal Reservoir Engineering. Stanford University, SGP-TR-227. URL: https://pangea.stanford.edu/ERE/db/GeoConf/papers/SGW/2024/Heeg.pdf.

Hubbard, P.G., Ou, R., Xu, T., Luo, L., Nonaka, H., Karrenbach, M., and Soga, K. (2022). Road deformation monitoring and event detection using asphalt-embedded distributed acoustic sensing (DAS). Structural Control Health Monitoring. URL: https://doi.org/10.1002/stc.3067.

Jousset, P., et al. (2018). Dynamic strain determination using fibre-optic cables allows imaging of seismological and structural features. Nature Communications, 9, 2509. DOI: https://doi.org/10.1038/s41467-018-04860-y

Lancelle, C. (2016). Distributed acoustic sensing for imaging near-surface geology and monitoring traffic at Garner Valley, California. Ph.D. dissertation. University of Wisconsin – Madison.

Lecocq, T., et al. (2020). Global quieting of high-frequency seismic noise due to COVID-19 pandemic lockdown measures. Science. 369(6509): 1338–1343. DOI: https/doi.org/10.1126/science.abd2438.

Li, Z., Zhang, J., Wang, M., Zhong, Y., and Peng, F. (2020). Fiber distributed acoustic sensing using convolutional long short-term memory network: a field test on high-speed railway intrusion detection, Optics Express, 28(3), 2925-2938. DOI: https://doi.org/10.1364/OE.28.002925.

Lindsey, N.J., Martin, E. R., Dreger, D. S., Freifeld, B., Cole, S., James, S. R., Biondi, B. L., and Ajo-Franklin, J. B. (2017). Fiber-Optic Network Observations of Earthquake Wavefields. Geophysical Research Letters, 44(23), 11,792-11,799. URL: https://doi.org/10.1002/ 2017GL075722.

Lindsey, N., Dawe, T., and Ajo-Franklin, J. (2019). Illuminating seafloor faults and ocean dynamics with dark fiber distributed acoustic sensing. Science, 366, 1103–1107. URL: https://doi.org/10.1126/science.aay5881.

Lindsey, N.J., Yuan, S., Lellouch, A., Gualtieri, L., Lecocq, T., and Biondi, B. (2020). City-scale dark fiber DAS measurements of infrastructure use during the COVID-19 pandemic. Geophysical Research Letters, 47(16): e2020GL089931. URL: https://doi.org/10.1029/2020GL089931.

Lord, N., Wang, H., and Fratta, D. (2016). A Source-Synchronous Filter for Uncorrelated Receiver Traces from a Swept-Frequency Seismic Source. Geophysics, 81, P47-P55. DOI: https://doi.org/10.1190/geo2015-0324.1.

Louie, J. N. (2001). Faster, Better: Shear-Wave Velocity to 100 Meters Depth from Refraction Microtremor Arrays. Bulletin of the Seismological Society of America, 91 (2), 347–364. DOI: https://doi.org/10.1785/0120000098.

Masciotta, M., Barontini, A., Ramos, L., Mendes, P., and Lourenco, P. (2018). An Overview on Structural Health Monitoring: From the Current State-of-the-Art to New Bio-inspired Sensing Paradigms. International Journal of Bio-Inspired Computation. 14(1), 1–26. URL: https://core.ac.uk/download/pdf/185628712.pdf.

Mateeva, A., Lopez, J., Potters, H., Mestayer, J., Cox, B., Kiyashchenko, D., Wills, P., Grandi, S., Hornman, K., Kuvshinov, B., Berlang, W., Yang, Z., and Detomo, R. (2014). Distributed acoustic sensing for reservoir monitoring with vertical seismic profiling. Geophysical Prospecting, 62(4), 679–692. URL: https://doi.org/10.1111/ 1365-2478.12116

McDaniel, A., Fratta, D., Tinjum, J. M., and Hart, D. J. (2018). Long-term district-scale geothermal exchange borefield monitoring with fiber optic distributed temperature sensing. Geothermics, 72, 193–204. URL: https://doi.org/10.1016/j.geothermics.2017.11.008.

Okabe, Y., and Wu, Q. (2016). Using optical fibers for ultrasonic damage detection in aerospace structures. Structural Health Monitoring (SHM) in Aerospace Structures, 95–118. URL: https://doi.org/10.1016/ B978-0-08-100148-6.00004-4.

Parker T., Shatalin S., and Farhadiroushan M. (2014). Distributed Acoustic Sensing - A new tool for seismic applications. First Break. 32:61–69. DOI: https://doi.org/10.3997/1365-2397.2013034.

Patterson, J.R., Cardiff, M., Coleman, T.I., Wang, H.F., Feigl, K.L., Akerley, J., and Spielman, P. (2017). Geothermal reservoir characterization using distributed temperature sensing at Brady Geothermal Field, Nevada.: Geophysics, 36. URL: https://doi.org/10.1190/tle36121024a1.1.

Pierce, S.G., Philp, W.R., Culshaw, B., Gachagan, A., McNab, A., Hayward, G., and Lecuyer, F. (1996). Surface-bonded optical fibre sensors for the inspection of CFRP plates using ultrasonic Lamb waves. Smart Materials and Structures, 5(6), 776–787. URL: https://doi.org/10.1088/0964-1726/5/6/007.

Sayde, C., Gregory, C., Gil-Rodriguez, M., Tufillaro, N., Tyler, S., Giesen, N. van de, English, M., Cuenca, R., and Selker, J. S. (2010). Feasibility of soil moisture monitoring with heated fiber optics. Water Resources Research, 46(6). URL: https://doi.org/10.1029/2009WR007846.

Selker, J.S., Thévenaz, L., Huwald, H., Mallet, A., Luxemburg, W. van de Giesen, N., Stejskal, M., Zeman, J., Westhoff, M., and Parlange M.B., (2006). Distributed fiber-optic temperature sensing for hydrologic systems. Water Resour. Res., 42(12), W12202. URL: https://doi.org/10.1029/2006WR005326.

Stokoe, K.H., II, Wright, S.G., Bay, J.A. and Roesset, J.A. (1994). Characterization of geotechnical sites by SASW method. Geophysical Characterization of Sites, Technical Committee for X111 ICSMFE, A.A. Balkema Publisher, Rotterdam, Netherlands, 785-816.

Tanimola, F. and Hill, D. (2009). Distributed fibre optic sensors for pipeline protection. Journal of Natural Gas Science and Engineering, 1(4–5), 134-143. URL: https://doi.org/10.1016/j.jngse.2009.08.002.

Vantassel, J.P, Cox, B.R., Hubbard, P.G., and Yust, M. (2022b). Extracting high-resolution, multi-mode surface wave dispersion data from distributed acoustic sensing measurements using the multichannel analysis of surface waves, Journal of Applied Geophysics, 205, URL: https://doi.org/10.1016/ j.jappgeo.2022.104776.

Vantassel, J.P., Cox, B.R., Menq, F., Hubbard, P., Yust, M., and Fratta, D. (2022a). Distributed Acoustic Sensing for Extracting High-Resolution, Multi-Mode Surface Wave Dispersion Data using Multi-channel Analysis of Surface Waves. 4th International Conference on Performance-based Design in Earthquake Geotechnical Engineering (PDBIV). Beijing, China.

Wang, H.F., Zeng, X., Miller, D. E., Fratta, D., Feigl, K.L., Thurber, C.H., and Mellors, R.J. (2018). Ground motion response to an ML 4.3 earthquake using co-located distributed acoustic sensing and seismometer arrays. Geophysical Journal International, 213(3): 2020-2036. URL: https://doi.org/10.1093/gji/ggy102.

Yokogawa (2013). World Pipelines, 'Why use a DTS system? Yokogawa Europe Corporation. URL: https://www.yokogawa.com/eu/library/resources/media-publications/world-pipelines-why-use-a-dts-system/

Youd, T.L., Bartholomew, H., and Proctor, J. (2004). Geotechnical Logs and data from permanently instrumented field sites: Garner Valley Downhole Array (GVDA) and Wildlife Liquefaction Array (WLA), UCSB Internal Report, URL: http://nees.ucsb.edu/gvda-geodata/geotech-data-report.pdf.

Yu, C., Zhan, Z., Lindsey, N. J., Ajo-Franklin, J. B., and Robertson, M. (2019). The Potential of DAS in Teleseismic Studies: Insights From the Goldstone Experiment. Geophysical Research Letters, 46(3), 1320–1328. URL: https://doi.org/10.1029/2018GL081195.

Zeng, X., Thurber, C., Wang, H., Fratta, D., and Feigl, K. (2022b). "High-resolution Shallow Structure at Brady Hot Springs Using Ambient Noise Tomography (ANT) on a trenched Distributed Acoustic Array (DAS) Array." Distributed Acoustic Sensing in Geophysics, Geophysical Monogram 268, 101-112, Edited by Y. Li, M. Karrenbach, and J. Ajo-Franklin. American Geophysical Union, John Wiley and Sons. DOI: https://doi.org/10.1002/9781119521808.ch08.

Zeng, X., Wang, H., Lord, N., Fratta, D., and Coleman, T. (2022a). "Field trial of Distributed Acoustic Sensing in an Active Room-and-Pillar

Mine." Distributed Acoustic Sensing in Geophysics, Geophysical Monogram 268, 67-80, Edited by Y. Li, M. Karrenbach, and J. Ajo-Franklin. American Geophysical Union, John Wiley, and Sons, DOI: https://doi.org/10.1002/9781119521808.ch05.

Zhang, G., Li, W., Qi, L., Liu, J., Song, Z., and Wang, J. (2018). Design of Wideband GHz Electric Field Sensor Integrated with Optical Fiber Transmission Link for Electromagnetic Pulse Signal Measurement. Sensors, Multidisciplinary Digital Publishing Institute, 18(9), 3167. URL: https://doi.org/10.3390/s18093167.

Zhu, J.C., Li, X. Y., Feng, Y. F., Zheng, H., Fang, J. W., Liu, S. C. (2019). Application of distributed optical fiber sensing technology in static test of bridge. Transportation Science and Technology, 2, 36-38.